Novel Trifluoromethyl-Containing Poly(amide–imide)s: Organosolubility, Optical Behavior, Thermostability, and Crystallinity

Hossein Behniafar, Narges Sefid-Girandehi, Mahdiyeh Hosseinpour

School of Chemistry, Damghan University, Damghan 36715-364, Iran

ABSTRACT: A new dicarboxylic acid monomer, 2,6-bis(1,3-dioxo-5-carboxyisoindolin-2-yl)-4,4′-bis(trifluoromethyl)-1,1′-diphenyl ether (IFDPE), bearing two preformed imide rings was synthesized via a three-step manner from 4-(trifluoromethyl)phenol and 4-chloro-3,5-dinitrobenzotrifluoride. The monomer IFDPE was then used to prepare a series of novel trifluoromethyl-containing poly(amide–imide)s via a direct phosphorylation polycondensation with various aromatic diamines. The intrinsic viscosities of the polymers were found to be in the range 0.86–1.02 d/g. The weight- and number-average molecular weights of the resulting polymers were determined with gel permeation chromatography. The polymeric samples were readily soluble in a variety of organic solvents and formed low-color, flexible thin films via solution casting. The values of the absorption edge wavelength were determined by ultraviolet–visible spectroscopy, and all of the resulting poly(amide–imide)s films exhibited high optical transparency. The resulting polymers showed moderately high glass-transition temperatures in the range 295–324°C and had 10% weight loss temperatures in excess of 524°C in nitrogen. The crystallinity extents were qualitatively investigated with wide-angle X-ray diffraction measurements. Scanning electron microscopy images revealed an agglomerated bulk with nonuniformity on the surface. © 2012 Wiley Periodicals, Inc. J Appl Polym Sci 000: 000–000, 2012

Key words: fluoropolymers; high performance polymers; high temperature materials; polyimides

INTRODUCTION

During recent years, considerable attention has been devoted to the preparation of new series of fluorine-containing high-performance polymers with a large variety of fluorinated monomers.[1–5] The exceptional results corresponding to the synthesis of processable fluoropolymers have become greater and greater over the course of time via the design of new chemical structures, and it seems that we have to continue this research line for the future. Fluoropolymers as a unique class of materials have a higher thermal stability, improved chemical resistance, and lower surface energy when compared to their nonfluorinated counterparts.[6–11] The introduction of a —CF₃ group, as the most prominent representative among perfluoro alkyl groups, into the aromatic structure of a high-performance polymer has been one of the most widely used strategies to enhance processability along with a desired set of properties for the resultant polymer.[12–18] This introduction modifies several physical properties; for example, it increases the solubility, thermal stability, optical transparency, and flame resistance. Simultaneously, it decreases the crystallinity, dielectric constant, water absorption, and color intensity. Moreover, because of the presence of —CF₃ substituents, the formation of a charge-transfer complex, which imparts a deep yellow color to the polymer, is largely hindered, and thus, the color intensity is considerably reduced. This makes the polyimide more suitable for some applications.

Two other key objects should be noted for better relation with this study. First, polymers with structurally hindered chains (the hindrance is caused by some local steric congestions along the chains) indicate improved processability relative to those lacking steric hindrance because of a constrained macromolecular twisting.[19–23] For instance, these congestions might be created by the presence of voluminous groups in the close positions of a chain. Second, among high-performance polymeric materials, an aromatic poly(amide–imide) seems to be a good compromise between thermostability and processability and can fill the gap formed between polyamides and polyimides.[24–28] A commercial product based on poly(amide–imide) materials is also available with Torlon. Accordingly, in this study, we dealt with the synthesis of a structurally hindered

imide-ring-containing fluorodiacid, 2,6-bis(1,3-dioxo-5-carboxyisoindolin-2-yl)-4,4′-bis(trifluoromethyl)-1,1′-diphenyl ether (IFDPE), via a three-step route from 4-(trifluoromethyl)phenol and 4-chloro-3,5-dinitrobenzotrifluoride. Indeed, the diacid IFDPE was designed as a potentially suitable monomer for poly(amide–imide)s, which was capable of imparting good processability and high thermal stability at the same time. The poly(amide–imide)s obtained from IFDPE were characterized by IR spectroscopy, NMR, intrinsic viscosity ([η]) measurements, gel permeation chromatography (GPC), thin-film characteristics, thermogravimetric analysis (TGA), differential scanning calorimetry (DSC), and organosolubility measurements.

EXPERIMENTAL

Materials

Trimellitic anhydride (TMA) and triphenyl phosphite (TPP) were purchased from Aldrich Chemical Co. (Switzerland) and were used as received without further purification. All of the other chemicals were purchased from Merck Chemical Co. (Germany) 4-(Trifluoromethyl)phenol and 4-chloro-3,5-dinitrobenzotrifluoride were used as received. 4,4′-Oxydianiline (ODA) was purified by recrystallization from ethanol before use. 4,4′-Diamino-2,2′-diphenyl-1,1′-diphenyl ether (APDPE) and 2,2′-bis(4-aminophenoxy)-1,1′-binaphthyl (BAPBN) were synthesized and purified by procedures reported elsewhere.[29,30] 2,6-Diamino-4,4′-bis(trifluoromethyl)-1,1′-diphenyl ether (AFDPE) was synthesized during the diacid monomer preparation course. Reagent-grade calcium chloride was dried *in vacuo* at 180°C before use. *N,N*-Dimethylacetamide (DMAc), *N,N*-dimethylformamide (DMF), dimethyl sulfoxide (DMSO), *N*-methyl-2-pyrrolidone (NMP), and pyridine were purified by distillation under reduced pressure over calcium hydride and stored over 4-Å molecular sieves. Hydrazine monohydrate and 10% palladium on activated carbon were used as received. Tetrahydrofuran (THF) and toluene were dried by sodium before use.

Measurements

The [η] data were measured with an Ubbelohde viscometer (Chaina) with polymer solutions in DMAc at 30°C. These values were measured at concentrations of 0.10, 0.25, and 0.50 g/dL in DMAc at 30°C and were plotted against the concentrations used, and linear extrapolation was done. The value of [η] was obtained as the *y*-axis intersect. In the other word, these values for all polymeric solutions were determined through the extrapolation of the concentrations used to zero.[31] The melting points were determined in open capillaries with an IA 9200 series

digital melting point apparatus (UK). Fourier transform infrared (FTIR) spectra were recorded on a Perkin-Elmer RX I FTIR spectrometer. The spectra of the solids were obtained with KBr pellets. ^{1}H-NMR spectra were recorded with a Bruker Avance 500 NMR instrument operated at 500 MHz in hexadeuterated dimethyl sulfoxide (DMSO-d_6) with tetramethylsilane as an internal standard. ^{13}C-NMR spectra were also obtained with the same apparatus operated at 125 MHz. TGA and DSC were performed on a Mettler TA 5000 system (Columbus, OH) under a nitrogen atmosphere at a heating rate of 10°C/min. The weight-average molecular weight (M_w) and number-average molecular weight (M_n) of the resulting poly(amide–imide)s were determined by GPC. This chromatography was done on a Waters 150-C instrument (USA) using Styragel columns and a differential refractometer detector. The molecular weight calibration was carried out with polystyrene standards. Calibration and measurements were made at a flow rate of 1 mL/min with THF as the eluent. The ultraviolet maximum wavelength (λ_{max}) values were determined with a GBC model 916 ultraviolet–visible (UV–vis) instrument (GBC Scientific Equipment, Australia) in DMSO at a concentration of 10^{-5} mol/L. The cut-off wavelength [absorption edge wavelength (λ_0)] values of the prepared thin films were determined with a Perkin-Elmer PTP-1 Peltier System Lambda 25 UV–vis spectrometer. Wide-angle X-ray diffraction (WAXD) patterns were obtained at room temperature with film specimens on a Bruker Avance D5 X-ray diffractometer with Ni-filtered Cu/Kα radiation (30 kV, 25 mA). The morphologies of the samples were determined with a Hitachi S-4160 scanning electron microscope.

Synthesis of 2,6-dinitro-4,4′-bis(trifluoromethyl)-1,1′-diphenyl ether (NFDPE)

In a three-necked, round-bottom flask equipped with a nitrogen inlet, 4-(trifluoromethyl)phenol (1.621 g, 10 mmol) and anhydrous potassium carbonate (2.902 g, 21 mmol) were suspended in a mixture of dry DMF (10 mL) and toluene (4 mL). The mixture was then refluxed at 140°C with a Dean–Stark trap to remove small amount of water azeotropically. After most of the toluene was distilled, 4-chloro-3,5-dinitrobenzotrifluoride (2.705 g, 10 mmol) was added when the mixture was cooled to 60°C. The mixture was then allowed to warm to 120°C and was kept at that temperature for 6 h. After it was cooled to 25°C, it was poured into 50 mL of CH_3OH/H_2O to give a yellow solid. After it was filtered under reduced pressure, the crude product was washed twice with hot water. After drying, the product was recrystallized from DMF/H_2O to give pale yellow fine crystals (76% yield, mp = 79–81°C).

FTIR (KBr, cm^{-1}): 1542, 1322 (—NO$_2$ stretch), 1267, 1252, 1182, 1141, 1099 (C—F and C—O stretch). ^{1}H-NMR (DMSO-d_6, δ, ppm): 8.43 (s, 2H, Ha), 7.88 (d, J = 8.6 Hz, 2H, Hc), 7.07 (d, J = 8.6 Hz, 2H, Hb). ^{13}C-NMR (DMSO-d_6, δ, ppm): 140.65 (C5), 138.79 (C4), 133.90 (C3), 132.12 (C2), 130.31 (C7), 129.22 (C*), 126.95 (C*), 125.91 (C6), 124.92 (C*), 123.78 (C1 and C8, quartet, $^2J_{C—F}$ = 35 Hz), 122.72 (C*).
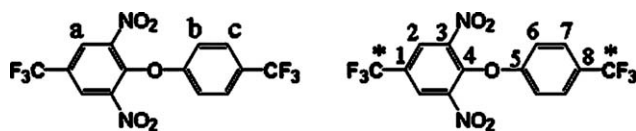
Synthesis of AFDPE

To a suspension of the purified dinitro compound (NFDPE; 3.96 g, 10 mmol) and 10% Pd/C (0.02 g) in ethanol (15 mL), hydrazine monohydrate (1.5 mL) was added dropwise to the stirred mixture at 70°C within 10 min. After complete addition, the mixture was heated at the reflux temperature for another 2 h. The reaction solution was filtered hot to remove Pd/C, and the filtrate was then filtered cold to remove the solvent. The crude product was purified by recrystallization from ethanol to give pale cream needles (69% yield, mp = 109–111°C).

FTIR (KBr, cm^{-1}): 3463, 3376 (N—H stretch), 1222, 1199, 1163, 1116 (C—F and C—O stretch). ^{1}H-NMR (DMSO-d_6, δ, ppm): 7.85 (d, J = 8.1 Hz, 2H, Hc), 7.03 (d, J = 8.1 Hz, 2H, Hb), 6.77 (s, 2H, Ha), 4.82 (s, 4H, Hd). ^{13}C-NMR (DMSO-d_6, δ, ppm): 152.54 (C4), 146.44 (C5), 140.91 (C3), 130.69 (C7), 129.33 (C2), 128.12 (C*), 125.68 (C1 and C8, quartet, $^2J_{C—F}$ = 35 Hz), 125.55 (C6 and C*), 123.64 (C*), 121.47 (C*).
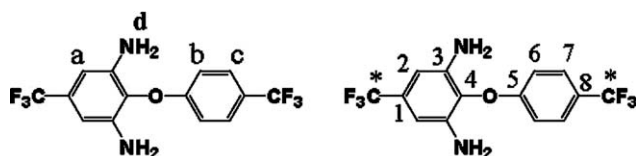

Synthesis of IFDPE

AFDPE (3.36 g, 10 mmol), TMA (4.80 g, 25 mmol), and glacial acetic acid (50 mL) were poured into a reaction flask. The heterogeneous mixture obtained was then refluxed under an N$_2$ atmosphere for 15 h. Next, the reaction mixture was filtered to give a yellow precipitate. The precipitate was washed several times with hot ethanol to remove acetic acid residue. The purification of the product obtained was performed by recrystallization from DMF/H$_2$O. The solid (IFDPE) was then dried under reduced pressure at 100°C for 24 h to afford dried yellow fine crystals (95% yield, mp = 365–368°C).

FTIR (KBr, cm^{-1}): 2400–3500 (acid O—H stretching), 1786 (imide, symmetric C=O stretching), 1737 (acid C=O stretching and asymmetric imide C=O

stretching), 1375 and 732 (imide-ring vibration, axial, transverse, and out of plane), 1256, 1224, 1127, 1103 (C—F and C—O stretching). ^{1}H-NMR (DMSO-d_6, δ, ppm): 13.80 (short and broad, 2H, acid H), 8.48 (dd, J = 7.7, J = 1.0 Hz, 2H, He), 8.39 (s, 2H, Hf), 8.16 (d, J = 7.7, 2H, Hd), 8.10 (s, 2H, Ha), 7.91 (d, J = 9.4 Hz, 2H, Hc), 7.44 (d, J = 9.4 Hz, 2H, Hb). ^{13}C-NMR (DMSO-d_6, δ, ppm): 166.01 (C15 and C16), 157.43 (C4), 151.38 (C5), 141.26 (C3), 136.63 (C14), 135.67 (C12), 133.85 (C11), 132.30 (C9), 131.01 (C7), 130.56 (C2), 129.70 (C13), 129.11 (C10), 128.02 (C*), 126.14 (C1 and C8, quartet, $^2J_{C—F}$ = 45 Hz), 125.91 (C6 and C*), 123.87 (C*), 122.10 (C*)
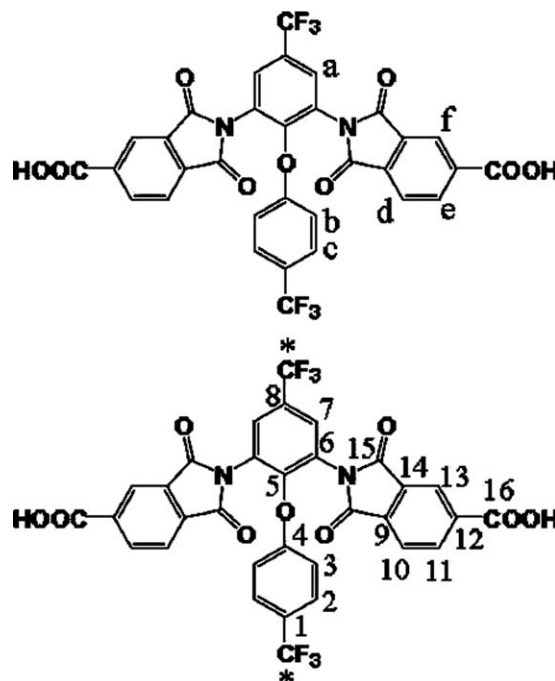
Preparation of the poly(amide–imide)s

A typical example of the TPP-activated polycondensation is described as follows. A mixture of IFDPE (0.684 g, 1 mmol), AFDPE (0.336 g, 1 mmol), CaCl$_2$ (0.2 g), pyridine (1.2 mL), TPP (0.6 mL), and NMP (5 mL) were heated with stirring at 100°C for 3 h. The viscosity of the reaction solutions increased after 1 h, and an additional 3.0 mL of NMP was added to the reaction mixture. At the end of the reaction, the obtained polymer solution was trickled into stirred methanol. The yellow stringy polymer was washed thoroughly with hot water and methanol, collected by filtration, and dried at 100°C under reduced pressure. The calculated yield was about 95%. [η] of the polymer obtained (IFDPE/AFDPE) was 0.86 dL/g, as measured at polymer concentrations of 0.10, 0.25, and 0.50 g/dL in DMAc at 30°C. The other poly(amide–imide)s were synthesized in a similar manner.
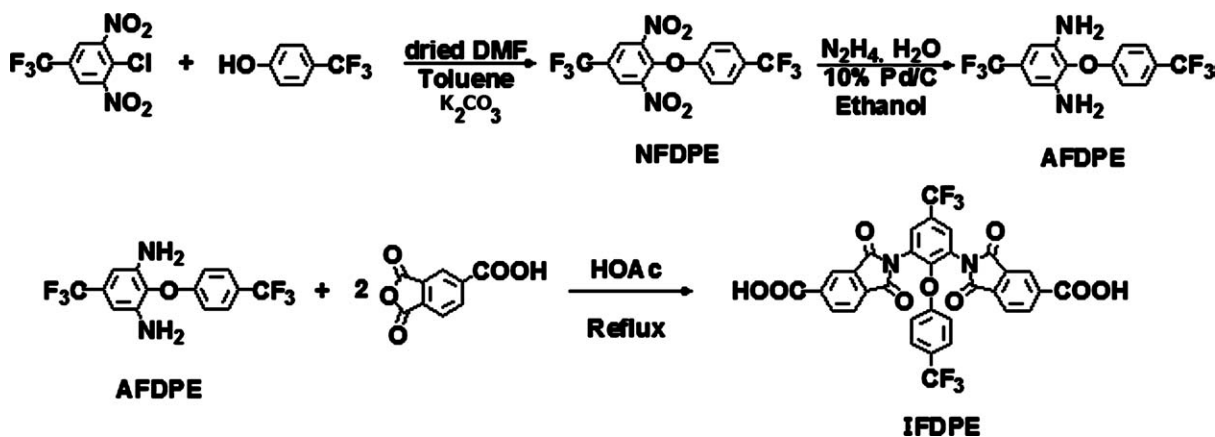
Scheme 1 Synthesis of the new monomer IFDPE (HOAc = acetic acid).

RESULTS AND DISCUSSION

Synthesis of diamine AFDPE

Scheme 1 shows the synthesis route used to prepare AFDPE by a two-step process. In the first step, aromatic nucleophilic displacement of 4-chloro-3,5-dinitrobenzotrifluoride with 4-(trifluoromethyl)phenol in the presence of anhydrous K_2CO_3 in DMF solvent; this resulted in NFDPE as a pale yellow solid. In the second step, this dinitro intermediate was reduced in ethanol in the presence of hydrazine hydrate and a catalytic amount of palladium on activated carbon at 80°C to produce white crystals of the fluorinated diamine AFDPE. The structures of dinitro NFDPE and diamine AFDPE were confirmed by IR and NMR spectroscopic methods. In the IR spectrum of dinitro NFDPE, the peaks attributed to the stretching vibrations of the bonds Ar—O and C—F appeared at 1267, 1252, 1182, and 1141 cm^{-1}. Moreover, the absorptions appearing around 1322 and 1542 cm^{-1} were due to the symmetric and asymmetric stretching of —NO_2 groups. In the ^{1}H-NMR spectrum of NFDPE, the existing three signals could be easily attributed to their appropriate hydrogens in the chemical formula. Here, two hydrogens attached to the nitro-group-containing ring (H_a) resulted in a singlet centralized at 8.43 ppm. Furthermore, in the ^{13}C-NMR spectrum, eight peaks corresponding to the eight kinds of aromatic carbons appeared in the range 123.8–140.6 ppm. In this spectrum, the quartets of the heteronuclear ^{13}C–^{19}F coupling appear in the region 122.7–129.2 ppm. The coupling constant of one-bond C—F was about 270 Hz, and that of the two-bond C—F was about 35 Hz. Thereby, all of these spectral patterns were thoroughly in agreement with the proposed structure of dinitro NFDPE. In the IR spectrum of the diamine AFDPE, the characteristic absorption of the nitro groups disappeared, and the characteristic bonds of the amino groups at 3463 and 3376 cm^{-1} (N—H stretching) and 1590 cm^{-1} (N—H bending) appeared after reduction. In the ^{1}H-NMR spectrum of diamine AFDPE, the signals of aromatic protons appeared in the range 6.77–7.85 ppm, and the characteristic resonance signal at 4.82 ppm was due to the amino group. In the ^{13}C-NMR spectrum of diamine AFDPE, the signals of the eight aromatic carbons appeared in the range 125.5–152.5 ppm. Moreover, the quartets of the heteronuclear ^{13}C–^{19}F coupling appeared in the region 121.5–128.1 ppm. The coupling constant of one-bond C—F was about 250 Hz, and that of the two-bond C—F was about 35 Hz.

Synthesis of the monomer IFDPE

Scheme 1 shows the synthetic route to the fluorinated diimide–diacid IFDPE by the ring-opening addition of diamine AFDPE and TMA in refluxing glacial acetic acid to yield the corresponding di(amic acid) intermediate, followed by the intramolecular cyclodehydration of this intermediate to give rise to the related cyclic imide groups. The FTIR spectrum of the monomer IFDPE showed the characteristic absorption bands around 2400–3500 cm^{-1} (—OH, carboxylic acid), 1786 cm^{-1} (imide C=O asymmetrical stretching), and 1737 cm^{-1} (imide C=O symmetric stretching and acid C=O stretching); this confirmed the presence of the imide-ring and carboxylic acid groups in the structure. In addition to the other aromatic hydrogens, the ^{1}H-NMR spectrum of IFDPE presented three proton signals around the downfield regions (8.16–8.48 ppm) due to the trimellitic acid moiety. Moreover, protons for the carboxylic acid groups were observed at about 13.80 ppm in the form of a short and broad peak. The ^{13}C-NMR spectrum of IFDPE exhibited 14 peaks of various absorptions for aromatic carbons. In this spectrum, the carbons of carboxylic acid and imide groups were observed at about 166.0 ppm.
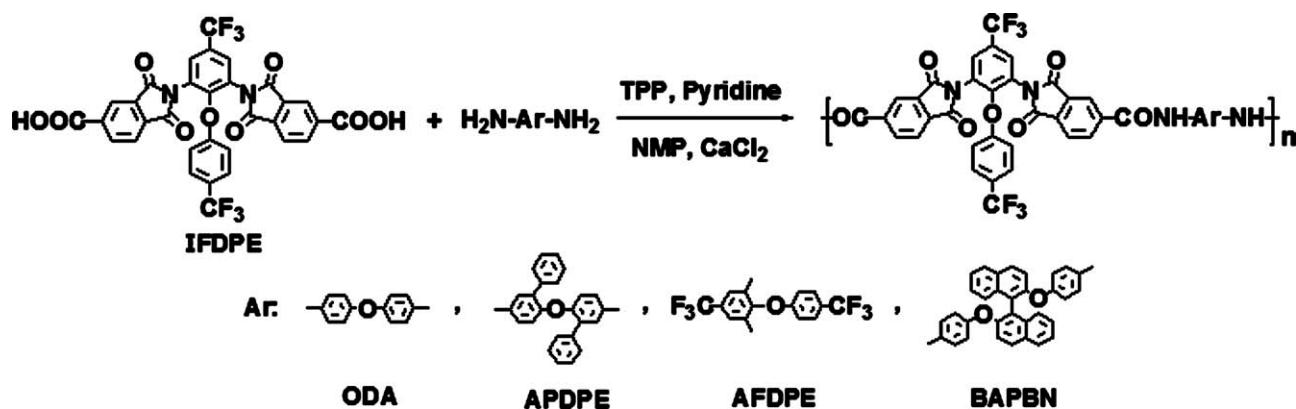
Scheme 2 Preparation of the poly(amide–amide)s.

Preparation of the fluorinated poly(amide–imide)s

According to the phosphorylation technique first described by Yamazaki and Higashi,[32] a series of novel poly(amide–imide)s were synthesized from the diacid IFDPE and various diamines, as shown in Scheme 2. All of the polycondensations were homogeneous throughout the reactions and afforded highly viscous polymer solutions with up to 90% yields. The [η] values of the resulting poly(amide–imide)s in DMAc at 30°C and the results of the GPC analyses were tabulated in Table I. The obtained polymers had [η] values in the range 0.86–1.02 dL/g. Furthermore, the poly(amide–imide)s IFDPE/AFDPE and IFDPE/BAPBN had polydispersity index (PDI) values of 2.10 and 1.91, respectively. The molecular weights of these polymers were high enough to obtain flexible and tough thin films through casting from their DMF solutions. The average molecular weights of the other two poly(amide–imide)s were not detectable because of their low solubility in the THF eluent. The formation of the poly(amide–imide)s was confirmed by FTIR and NMR spectroscopy methods. The FTIR spectra of the poly(amide–imide)s exhibited characteristic amide bands at about 3370 (N—H stretching) and 1630

(C=O stretching) cm^{-1}. The resulting polymers also showed characteristic imide bands around 1780 and 1730 cm^{-1} (asymmetrical and symmetrical C=O stretching vibrations, respectively) and 1340 (imide C—N stretching). In these spectra, the lack of the highly broad absorption peak in the region 2400–3500 cm^{-1}, related to acid O—H stretching, indicated that no any IFDPE monomer was present in the sample composition. Instead, in the left side of this region, a peak corresponding to N—H stretching appeared at about 3370 cm^{-1}, as stated. In the ^{1}H-NMR spectra of the resulting poly(amide–imide)s, the existing aromatic protons resonated in the region 6.9–8.5 ppm. Among the aromatic protons, the protons adjacent to the imide ring appeared at farthest downfield because of the resonance of the imide ring. Also, the signals appearing at the most downfield region, about 10.05 ppm, were attributed to the protons of the amide linkages. All of the data obtained from the FTIR and ^{1}H-NMR spectroscopy are also listed in Table II.

Organosolubility

The solubility behavior of the prepared poly(amide–imide)s was tested qualitatively in various organic solvents, and the results are listed in Table III. All of the polymers were readily soluble in high-polar solvents, such as DMSO, DMF, DMAc, and NMP, at room temperature. Such good organosolubility was

TABLE I
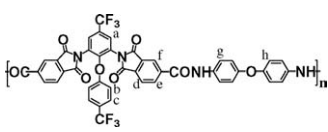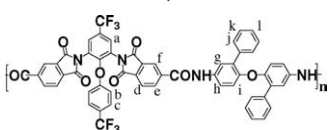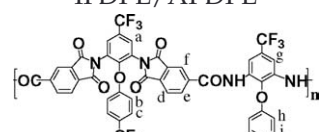**Some Characteristics of the Resulting Poly(amide–imide)s**
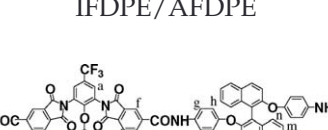
Polymer	Closed formula	[η] (dL/g)[a]	M_w[b]	M_n[b]	PDI
IFDPE/ODA	$(C_{44}H_{22}F_6N_4O_8)_n$ (848)$_n$	0.98	—[c]	—[c]	—[c]
IFDPE/APDPE	$C_{56}H_{30}F_6N_4O_8$ (1000)$_n$	1.02	—[c]	—[c]	—[c]
IFDPE/AFDPE	$C_{46}H_{20}F_{12}N_4O_8$ (984)$_n$	0.86	18,794	8948	2.10
IFDPE/BAPBN	$C_{64}H_{34}F_6N_4O_9$ (1116)$_n$	0.92	22,124	11,579	1.91

[a] Measured in DMAc at 30°C.
[b] Measured by GPC in THF with polystyrene as a standard.
[c] Polymer was insoluble in THF at room temperature.

<div align="center">

**TABLE II**
FTIR and ^{1}H-NMR Results of the Resulting Poly(amide–imide)s

</div>

Structure and code	Results[a]
IFDPE/ODA	FTIR (cm^{-1}): 3371 (w, br), 2915 (w, sh), 1781 (w, sh), 1731 (s, sh), 1630 (m, sh), 1587 (m, sh), 1499 (s, sh), 1441 (m, sh), 1339 (s, sh), 1242 (m, sh), 1207 (s, sh), 1165 (w, sh), 1122 (s, sh), 948 (m, sh), 799 (m, sh), 772 (m, sh), 728 (m, sh). ^{1}H-NMR (δ, ppm): 10.05 (2H, N—H), 8.42 (2H, H$_f$), 8.24–8.31 (4H, H$_e$ H$_d$), 7.54–7.61 (6H, H$_a$ H$_g$), 7.42 (2H, H$_c$), 6.96–7.04 (6H, H$_b$ H$_h$).
IFDPE/APDPE	FTIR (cm^{-1}): 3362 (w, br), 2931 (w, sh), 1780 (w, sh), 1729 (s, sh), 1619 (m, sh), 1591 (m, sh), 1501 (s, sh), 1447 (m, sh), 1342 (s, sh), 1238 (m, sh), 1211 (s, sh), 1159 (w, sh), 1119 (m, sh), 941 (m, sh), 843 (m, sh), 798 (m, sh), 781 (m, sh), 728 (s, sh). ^{1}H-NMR (δ, ppm): 10.02 (2H, N—H), 8.45 (2H, H$_f$), 8.21–8.28 (4H, H$_e$ H$_d$), 7.85 (2H, H$_g$), 7.48–7.55 (4H, H$_a$ H$_h$), 7.39–7.44 (6H, H$_c$ H$_j$), 7.32 (4H, H$_k$), 7.21 (2H, H$_l$), 6.94–7.03 (4H, H$_b$ H$_i$).
IFDPE/AFDPE	FTIR (cm^{-1}): 3375 (w, br), 2918 (w, sh), 1780 (w, sh), 1731 (s, sh), 1629 (m, sh), 1590 (m, sh), 1499 (s, sh), 1439 (m, sh), 1341 (s, sh), 1251 (m, sh), 1202 (s, sh), 1163 (w, sh), 1119 (s, sh), 953 (m, sh), 799 (m, sh), 775 (m, sh), 726 (m, sh). ^{1}H-NMR (δ, ppm): 10.03 (2H, N—H), 8.42 (2H, H$_f$), 8.25–8.33 (4H, H$_e$ H$_d$), 7.52–7.60 (4H, H$_a$ H$_g$), 7.44 (4H, H$_c$ H$_i$), 6.95–7.02 (4H, H$_b$ H$_h$).
IFDPE/BAPBN	FTIR (cm^{-1}): 3368 (w, br), 2922 (m, sh), 1779 (w, sh), 1728 (s, sh), 1628 (m, sh), 1588 (m, sh), 1500 (s, sh), 1449 (m, sh), 1341 (s, sh), 1241 (m, sh), 1205 (s, sh), 1120 (s, sh), 961 (m, sh), 843 (w, sh), 799 (m, sh), 772 (m, sh), 725 (m, sh). ^{1}H-NMR (δ, ppm): 10.05 (2H, N—H), 8.42 (2H, H$_f$), 8.23–8.31 (4H, H$_e$ H$_d$), 7.53–7.63 (12H, H$_a$ H$_g$ H$_j$ H$_k$ H$_n$), 7.44 (2H, H$_c$), 7.31 (2H, H$_m$), 7.20 (2H, H$_l$), 7.04 (2H, H$_i$), 6.95–7.01 (6H, H$_b$ H$_h$).

not seen even in our recently synthesized nonfluorinated aromatic poly(ether–amide)s[10] and poly(amide–imide)s.[29] For example, the solubility behaviors of a poly(ether-amide) prepared from diamine 2,2′-bis(3,4,5-trifluorophenyl)-4,4′-diaminodiphenyl ether (FPAPE) and terphthalic acid (TPA) (poly(ether-amide) FPAPE/TPA), as well as a poly(amide-imide) prepared from diacid 2,2′-diphenyl-4,4′-bis(N-trimellitoyl)diphenyl ether (PTPE) and ODA (poly(amide-imide) PTPE/ODA), whose chemical structures are shown as follows, are tabulated in rows 5 and 6 of Table III for comparison.

FPAPE/TPA   **PTPE/ODA**
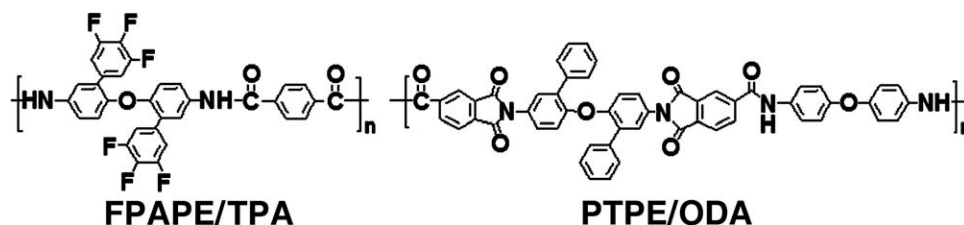
The poly(amide–imide)s IFDPE/AFDPE and IFDPE/BAPBN dissolved even in pyridine as a moderate polar solvent at room temperature. These two structurally well-designed polymers were thoroughly soluble in THF upon heating at about 70°C. As mentioned earlier, steric congestions of the chains, caused by the presence of trifluoromethylated phenoxy groups and their two lateral imide rings, resulted in local noncoplanarities along the chains, and consequently, excellent solubility was observed in a wide spectrum of organic solvents. Moreover, the presence of two additional CF$_3$ groups per repeat unit in the poly(amide-amide) IFDPE/AFDPE as well as the participation of twisted binaphthyl rings in the poly(amide–amide) IFDPE/BAPBN noticeably increased their organosolubility relative to the other two. In general, the excellent organosolubility of these polymers could be attributed to a combination of steric and electronic effects. The bulky CF$_3$-containing phenoxy pendant groups attached to the CF$_3$-containing backbone inhibited the close packing of the macromolecular chains and endowed a large amount of polarity because of the high electronegativity of the fluorine

TABLE III
Solubility of the Resulting Poly(amide–imide)s

Polymer	DMSO	DMF	DMAc	NMP	Py	THF	Tol
IFDPE/ODA	++	++	++	++	+	—	—
IFDPE/APDPE	++	++	++	++	+	+	—
IFDPE/AFDPE	++	++	++	++	++	++	—
IFDPE/BAPBN	++	++	++	++	++	++	—
FPAPE/TPA[a]	+	+	+	+	+	—	—
PTPE/ODA[b]	++	++	++	+	+	+	—

Py, pyridine; Tol, toluene; ++, soluble at room temperature; +, soluble on heating; —, partially soluble or insoluble.
[a]Data obtained from ref. 10.
[b]Data obtained from ref. 29.

atoms, and thereby, these fluoropoly(amide–imide)s showed good organosolubility, particularly in polar solvents.

Film characteristics and optical properties

λ_{max} of all of the polymers solutions with concentrations of 10^{-5} mol/L in DMSO appeared at about 305 nm (Table IV); this showed a relatively small energy band gap for the $\pi \rightarrow \pi^*$ transition. Reasonably, this could be attributed to the all-aromatic structures possessing phenyl pendant groups attached to the main-chain aromatic rings. To prepare a crack-free and homogeneous thin film, solutions of the polymers were made by the dissolution of about 0.50 g of the sample in 6 mL of DMF. These solutions were poured into a 5-cm glass Petri dish, which was heated *in vacuo* at 100°C for 3 h, 120°C for 6 h, and 150°C for 5 h to evaporate the solvent slowly. By being soaked in distilled water, the flexible and transparent thin films with almost no color were self-stripped from the glass surface. The obtained films were then used to investigate the optical properties of the poly(amide–imide)s. The plateau region of the UV–vis absorption spectrum of the resulting

TABLE IV
Film Characteristics and Optical Behavior of the Resulting Poly(amide–imide)s

Polymer	λ_{max} (nm)[a]	Film characteristics[b]	λ_0 (nm)[c]
IFDPE/ODA	308	Transparent, flexible, buff	382
IFDPE/APDPE	305	Transparent, flexible, pale yellow	389
IFDPE/AFDPE	306	Transparent, slightly brittle, cream colored	385
IFDPE/BAPBN	307	Transparent, flexible, pale yellow	394

[a] Obtained from dilute solutions with a polymer concentration of 10^{-5} mol/L in DMSO.
[b] The film thickness was about 50 μm.
[c] The point at which the light transmittance from the prepared thin films became less than 1%.

poly(amide–imide)s were extended to about 500 nm (Figure 1). Furthermore, the λ_0 values were determined at about 385 nm. These indicators clearly showed that the resultant thin films enjoyed a high level of optical transparency in the UV–vis light region. The spectra of the poly(amide–imide) films were nearly identical with each other. Table IV lists the values of λ_{max} obtained from the diluted solutions of the polymers in DMSO, the characteristics of the resulting films, and the values of the absorption edge.

DSC measurements

DSC was used to determine the glass-transition temperature (T_g) values of the samples obtained with a heating rate of 10°C/min under nitrogen. Figure 2 (top) shows a typical DSC thermogram of the poly(amide–imide) IFDPE/APDPE. The T_g values were read at the middle of the first breakdown observed in the DSC plots and was found to be in the range 295–324°C. In general, molecular packing and chain rigidity are among the main factors affecting T_g values. In the polymer IFDPE/AFDPE, the increased rotational barrier caused by the additional —CF$_3$ substituents of diamine AFDPE enhanced the T_g values relative to those of the polymer IFDPE/ODA up to 20°C. Further rotational barriers and, consequently, the T_g values could be observed by the incorporation of rigid and kinked binaphthyl units into the polymer IFDPE/BAPBN chains. Therefore,
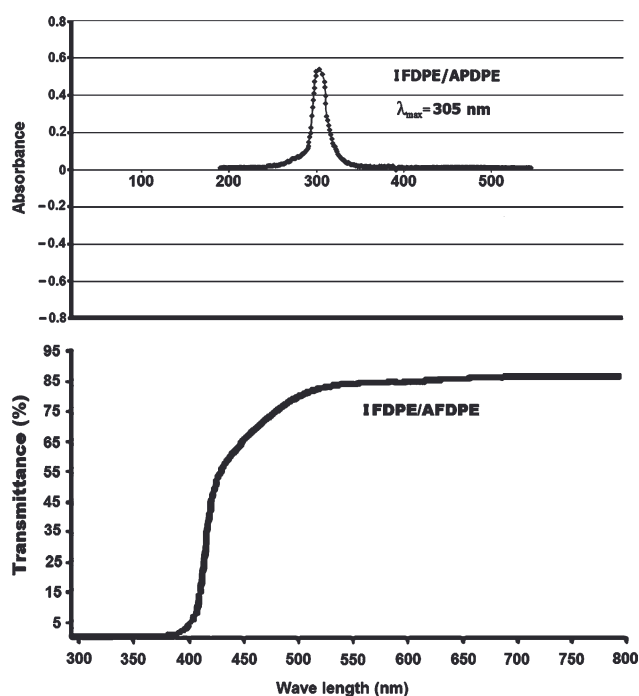

Figure 1 Molar absorptivity spectrum of the polymer IFDPE/APDPE solution (top). UV–vis transmission spectrum of the polymer IFDPE/AFDPE film (bottom).
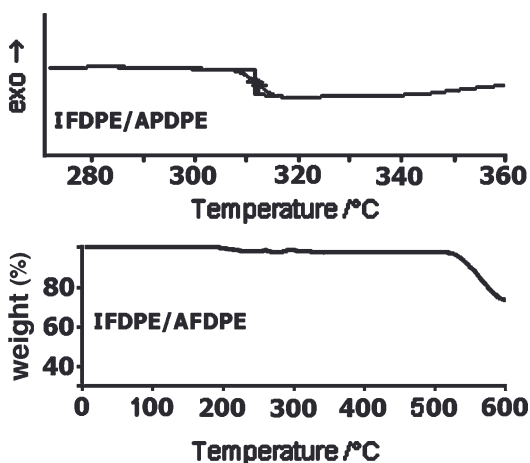
Figure 2 DSC thermogram of the polymer IFDPE/APDPE (top) and TGA thermogram of the polymer IFDPE/AFDPE (bottom).

in addition to the diacid IFDPE, the values of T_g were affected by diamine moieties, too; this showed the order BAPBN > AFDPE > APDPE > ODA, as illustrated in Table V. The poly(amide–imide)s possessing entirely voluminous substituents, that is, IFDPE/BAPBN and IFDPE/AFDPE, showed higher T_g values relative to the other two, that is, IFDPE/APDPE and IFDPE/ODA. As was expected, enhanced stiffness and bulkiness in the structures of the former two poly(amide–imide)s compared with the latter two restricted the free rotation of their main chains and, consequently, increased their T_g values. In addition, these fluorinated poly(amide–imide)s had higher and lower T_g values compared to our recently prepared aromatic poly(ether–amide)s and poly(amide–imide)s, respectively. For example, in a comparison between rows 1, 5, and 6 of Table V, it is obvious that the poly(amide–imide) IFDPE/ODA had a higher T_g value (up to 55°C) than the poly(ether–amide) FPAPE/TPA and a lower T_g value (up to 50°C) than the poly(amide–imide) PTPE/ODA.

Thermostability

The thermostability of the resulting poly(amide–imide)s were evaluated by TGA under a nitrogen atmosphere at a heating rate of 10°C/min, and the corresponding temperatures of 5 and 10% weight loss ($T_{5\%}$ and $T_{10\%}$, respectively) were all determined from the original TGA curves. All of the aromatic poly(amide–imide)s exhibited good thermal stability with insignificant weight loss up to 550°C in nitrogen. The $T_{5\%}$ and $T_{10\%}$ values of the poly(amide–imide)s stayed within 509–532 and 524–546°C, respectively. The amount of carbonized residue (char yield) of these polymer in a nitrogen atmos-

phere was up to 70% at 600°C. The high char yields of these polymers could be ascribed to their high aromatic content. Obviously, the data from thermal analysis showed that these poly(amide–imide)s had a fairly high thermal stability. Furthermore, the poly(amide–imide) derived from the fluorinated diamine AFDPE was somewhat more stable toward heat than those of derived from the other diamine comonomers. Typical TGA curves of the representative poly(amide–imide) IFDPE/AFDPE are shown in Figure 2 (bottom). In addition, the results obtained from these analyses are entirely tabulated in Table V. A higher thermostability was observed for this class of polymers compared to those for their non-fluorinated counterparts. For example, in a comparison between rows 1, 5, and 6 of Table V, it could be clearly concluded that the poly(amide–imide) IFDPE/ODA had a greater heat resistance relative to both poly(ether–amide) FPAPE/TPA (50–70°C) and poly(amide–imide) PTPE/ODA (20–30°C).

X-ray diffraction (XRD) studies

The crystallinities of poly(amide–imide)s IFDPE/ODA and IFDPE/APDPE were measured by WAXD at room temperature. The typical XRD patterns for these representative CF_3-containing polymers with 2θ values ranging from 5 to 50° are displayed in Figure 3. The obtained diffractograms obviously showed that the mentioned poly(amide–imide)s were essentially amorphous, and no remarkable crystal diffraction appeared in their WAXD curves. Apparently, the laterally attached trifluoromethylated phenoxy groups

TABLE V
Thermal Behavior of the Resulting Poly(amide–imide)s

Polymer	T_o (°C)[a]	T_g (°C)[b]	$T_{d5\%}$ (°C)[c]	$T_{d10\%}$ (°C)[d]	CY (wt %)[e]
IFDPE/ODA	292	295	509	538	71
IFDPE/APDPE	309	312	517	524	69
IFDPE/AFDPE	311	315	532	546	74
IFDPE/BAPBN	317	324	528	545	68
FPAPE/TPA[f]	233	239	456	467	—
PTPE/ODA[g]	337	345	479	520	69

[a] Onset temperature from DSC measurements in N_2, defined as the point at which the first deviation from the baseline on the low-temperature side was observed.
[b] T_g values from the DSC traces in N_2 at a heating rate of 10°C/min.
[c] Determined by TGA in N_2 at a heating rate of 10°C/min.
[d] Determined by TGA in N_2 at a heating rate of 10°C/min.
[e] CY, char yield. The residual weight percentages at 600°C determined by TGA in N_2 at a heating rate of 10°C/min.
[f] Data obtained from ref. 10.
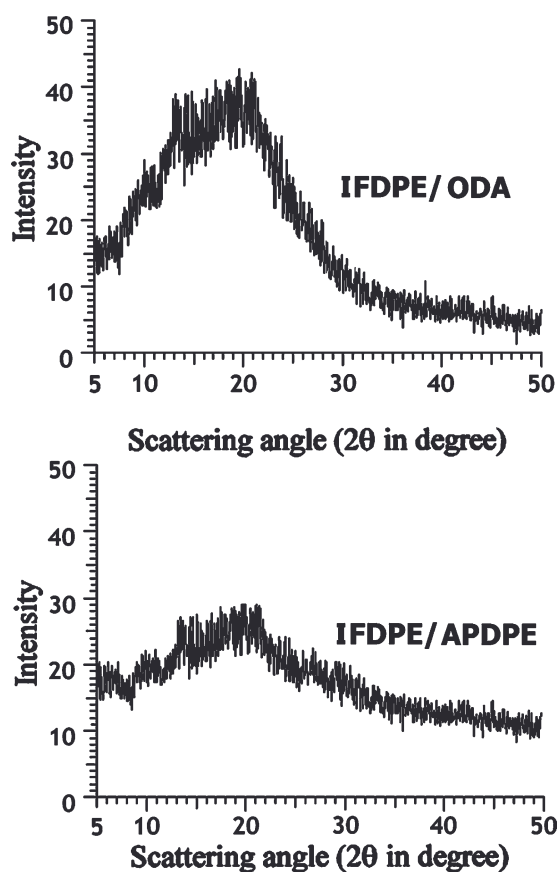[g] Data obtained from ref. 29.

Figure 3 XRD patterns of the polymers IFDPE/ODA (top) and IFDPE/APDPE (bottom).

interfered with packing efficiency and decreased the chain–chain interactions; this resulted in a decreasing crystallinity. Moreover, the effect of the diamine comonomers on the crystallinity amount could be observed by comparison of the unequal shapes of the diffractograms obtained. Accordingly, in addition to the imide-containing diacid monomer (IFDPE), the diamine comonomers, too, had somewhat of an effect on the amorphous nature of the final polymers. The crystallinity amount of poly(amide–imide) IFDPE/ODA was somewhat greater than that of poly(amide–imide) IFDPE/APDPE because of further macromolecular prevention of the diamine moiety against compactness for the later polymer in comparison with the former one.

Surface morphology

Figure 4 shows the scanning electron microscopy (SEM) images of poly(amide-imide)s IFDPE/ODA (top) and IFDPE/AFDPE (bottom). These SEM images clearly showed an agglomerated bulk with nonequal packing. In fact, these images revealed an amorphous morphology with nonuniformity in the surface area of the samples. This kind of surface

morphology might have been due to the same amorphous microstructures caused by the bulky CF$_3$-containing phenoxy lateral groups. Furthermore, the creation of local noncoplanarity and, consequently, local twisting along the main chains due to two bulky 1,3-dioxo-5-carboxyisoindolin-2-yl units and middle-sited trifluoromethylated phenoxy groups could have destroyed the regularity of the chains and caused a nonuniformity in the surface.

CONCLUSIONS

A structurally well-designed diacid (IFDPE) bearing CF$_3$ groups, ether hinges, and preformed imide rings was successfully synthesized. Next, a novel class of aromatic fluorinated poly(amide–imide)s were readily prepared from IFDPE and various aromatic diamines through direct phosphorylation polycondensation. The incorporation of voluminous and polar CF$_3$ lateral substituents along the macromolecular chains considerably increased their organosolubility and optical transparency. All of the polymeric low-colored thin films were highly flexible and showed high optical transparency in the UV–vis light region.
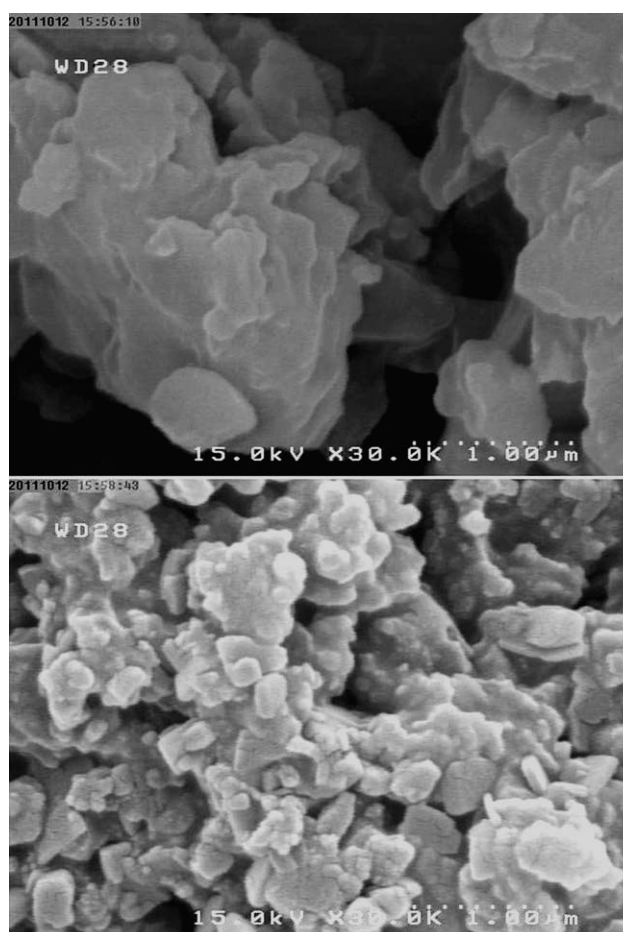

Figure 4 SEM images of the poly(amide–imide)s IFDPE/ODA (top) and IFDPE/AFDPE (bottom).

In sum, these fluoro-containing poly(amide–imide)s displayed good film-forming capability, excellent organosolubility, low crystallinity, reasonable thermal stability, and T_g values suitable for thermoforming processing.

References

1. Ma, T.; Zhang, S.; Li, Y.; Yang, F.; Gong, C.; Zhao, J. J Fluorine Chem 2010, 131, 724.
2. Shundrina, I. K.; Vaganova, T. A.; Kusov, S. Z.; Rodionov, V. I.; Karpova, E. V.; Malykhin, E. V. J Fluorine Chem 2011, 132, 207.
3. Zhu, Y.; Zhao, P.; Cai, X.; Meng, W. D.; Qing, F. L. Polymer 2007, 48, 3116.
4. Maji, S.; Banerjee, S. J Appl Polym Sci 2008, 108, 1356.
5. Han, X.; Tian, Y.; Wang, L.; Xiao, C.; Liu, B. Eur Polym J 2007, 43, 4382.
6. Garcia, J. M.; Garcia, F. C.; Serna, F.; de la Penta, J. L. Prog Polym Sci 2010, 35, 623.
7. Marchildon, K. Macromol React Eng 2011, 5, 22.
8. Ma, C. X.; Sheng, S. R.; Wei, M. H.; He, W.; Song, C. S. J Appl Polym Sci 2010, 118, 2959.
9. Hariharan, R.; Sarojadevi, M. Polym Int 2007, 56, 22.
10. Behniafar, H.; Sedaghatdoost, M. J Fluorine Chem 2011, 132, 276.
11. Liaw, D. J.; Huang, C. C.; Chen, W. H. Polymer 2006, 47, 2337.
12. Wang, X. L.; Li, Y. F.; Gong, C. L.; Ma, T.; Yang, F. C. J Fluorine Chem 2008, 129, 56.
13. Ghosh, A.; Banerjee, S. High Perf Polym 2009, 21, 173.
14. Liu, Y.; Zhang, Y.; Guan, S.; Li, L.; Jiang, Z. Polymer 2008, 49, 5439.
15. Yang, C. P.; Chen, R. S.; Chen, K. H. Colloid Polym Sci 2003, 281, 505.
16. Choi, H.; Chung, I. S.; Hong, K.; Park, C. E.; Kim, S. Y. Polymer 2008, 49, 2644.
17. Banerjee, S.; Madhra, M. K.; Salunke, A. K.; Maier, G. J Polym Sci Part A: Polym Chem 2002, 40, 1016.
18. Dasgupta, B.; Sen, S. K.; Maji, S.; Chatterjee, S.; Banerjee, S. J Appl Polym Sci 2009, 112, 3640.
19. Jang, W.; Shin, D.; Choi, S.; Park, S.; Han, H. Polymer 2007, 48, 2130.
20. Qiu, Z.; Chen, G.; Zhang, Q.; Zhang, S. Eur Polym J 2007, 43, 194.
21. Liaw, D. J.; Wang, K. L.; Chang, F. C. Macromolecules 2007, 40, 3568.
22. Mi, Q.; Ma, Y.; Gao, L.; Ding, M. J Polym Sci Part A: Polym Chem 1999, 37, 4536.
23. Chung, C. L.; Lee, W. F.; Lin, C. H.; Hsiao, S. H. J Polym Sci Part A: Polym Chem 2009, 47, 1756.
24. Buch, P. R.; Reddy, A. V. R. Polymer 2005, 46, 5524.
25. Behniafar, H.; Haghighat, S. Eur Polym J 2006, 42, 3236.
26. Bhuvana, S.; Sarojadevi, M. J Polym Res 2007, 14, 261.
27. Behniafar, H.; Beit-Saeed, A.; Hadian, A. Polym Degrad Stab 2009, 94, 1991.
28. Mallakpour, S.; Rafiemanzelat, F. Eur Polym J 2005, 41, 2945.
29. Behniafar, H.; Abedini-pozveh, A. Polym Degrad Stab 2011, 96, 1327.
30. Banihashemi, A.; Behniafar, H. Polym Int 2003, 52, 1136.
31. Braun, D.; Cherdron, H.; Rehahn, M.; Ritter, H.; Voit, B. Polymer Synthesis: Theory and Practice; Springer: Berlin, 2005; p 104.
32. Yamazaki, N.; Higashi, F. Tetrahedron 1974, 30, 1323.